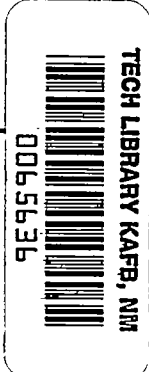# NATIONAL ADVISORY COMMITTEE
FOR AERONAUTICS

TECHNICAL NOTE 2374

EFFECT OF INITIAL MIXTURE TEMPERATURE ON

FLAME SPEED OF METHANE-AIR, PROPANE-AIR

AND ETHYLENE-AIR MIXTURES

By Gordon L. Dugger

Lewis Flight Propulsion Laboratory
Cleveland, Ohio

Washington
May 1951

NATIONAL ADVISORY COMMITTEE FOR AERONAUTICS

TECHNICAL NOTE 2374

EFFECT OF INITIAL MIXTURE TEMPERATURE ON FLAME SPEED OF

METHANE-AIR, PROPANE-AIR, AND ETHYLENE-AIR MIXTURES

By Gordon L. Dugger

SUMMARY

Flame speeds based on the inner edge of the shadow cast by the laminar Bunsen cone were determined for methane-air and ethylene-air mixtures as functions of composition at initial mixture temperatures ranging from 34° to 344° C. The data showed that flame speed increased with temperature at an increasing rate, as did similar data reported earlier for propane and air. The flame speeds were found to be affected by temperature on the basis of percentage in the decreasing order, methane, propane, and ethylene. The flame speed u for none of these fuels was exactly proportional to a power of initial temperature T_0; however, approximate equations for flame speed in centimeters per second (based on inner edge of shadow) for use in the temperature range 34° to 344° C were determined to be as follows:

For methane,

$$u = 0.000780 \ T_0^{1.89}$$

for propane,

$$u = 0.00246 \ T_0^{1.72}$$

and for ethylene,

$$u = 0.00971 \ T_0^{1.565}$$

Part of the data were recomputed on the basis of the surface indicated by the outer edge of the shadow cast by the flame cone. For a given fuel, the ratio of outer-edge value to inner-edge value was constant with respect to both temperature and composition, within the accuracy of the outer-edge measurements. Flame speeds calculated from the preceding empirical equations could therefore be converted to outer-edge values by multiplying by the constants 0.900, 0.885, and 0.849 for

methane, propane, and ethylene, respectively. Outer-edge values (room temperature) were close to values obtained from the visible Bunsen cone and from tube measurements.

The observed effect of temperature on flame speed for each of the fuels was reasonably well predicted by either the thermal theory as presented by Semenov or the square-root law of Tanford and Pease. The importance of active radicals in flame propagation was indicated by a simple linear relation between maximum flame speed and equilibrium radical concentrations for all three fuels. Equally good correlations resulted from using either hydrogen-atom concentration alone or a summation of effective relative concentrations of hydrogen atoms, hydroxyl radicals, and oxygen atoms and using either flame temperatures based on a sodium D-line measurement for a room-temperature mixture or adiabatic flame temperatures.

INTRODUCTION

The flame speed, or normal burning velocity, of a fuel-air mixture is a fundamental property governing flame propagation, which is one of the several major processes occurring in combustion equipment for flight propulsion. Inasmuch as plots of the performance data of aircraft combustors show that the combustion efficiency is related to the combustor-inlet temperature (for example, references 1 and 2), knowledge of how temperature affects the fundamental combustion properties of the fuel-air mixture is desirable. Consequently, as part of the combustion research program at the NACA Lewis laboratory, an investigation was initiated to study the effect of initial mixture temperature on flame propagation. The effect of temperature on flame speeds and stability limits of propane-air flames is reported in reference 3. An extension of the flame-speed phase of this investigation to include the effect of temperature on methane-air and ethylene-air flames is reported herein.

Previous work (reference 3) showed that the flame speed of propane-air mixtures increased with temperature at an increasing rate. It was shown that the thermal theory of flame propagation, as presented by Semenov in reference 4 for bimolecular reactions, predicted the effect of initial mixture temperature on the maximum flame speed of propane-air mixtures within approximately 5 percent. It was further shown that the square-root law of Tanford and Pease (references 5 and 6), which is based on the diffusion of active particles, predicted relative increases in maximum flame speed that were as much as 35 percent lower than the experimental results. Subsequent reevaluation of the temperature dependence predicted by the square-root law has shown, however, that the relative increases predicted by this theory for propane are within 14 percent of the experimental results.

2144

        Inasmuch as the activation energy of the oxidation process is an
important factor in the thermal-theory equations, it was decided to
obtain flame-speed - temperature data for a gaseous fuel having an
activation energy appreciably different from that of propane. Methane
was selected because it has an activation energy of 52 kilocalories per
gram-mole (from unpublished data obtained by A. D. Walsh, Leeds Univer-
sity, England), compared with 38 kilocalories per gram-mole for propane
(reference 7, p. 437).

        It was also thought that data for ethylene, which has shown anoma-
lous behavior in other correlations (reference 8) when compared with
other hydrocarbons, would be of value. The activation energy of ethyl-
ene, which is approximately 40 kilocalories per gram-mole (reference 9),
does not differ much from that of propane.

        The present report contains the results of a study of the effect
of initial mixture temperature over the range of 34° to 344° C on the
laminar flame speeds of methane-air and ethylene-air mixtures. The
flame speeds were computed from measurements based on the inner edge of
the shadow cast by the Bunsen cone; the shadowgraphs were obtained with
a parallel-beam shadowgraph system. The flame-speed values thus
obtained are compared with values obtained by other methods.

        Methane, propane, and ethylene are compared on the basis of rela-
tive increase in flame speed with initial temperature. A comparison
is also made among the experimental data for each fuel and the relative
effects of temperature on flame speed predicted by the thermal and
diffusion theories.

<center>SYMBOLS</center>

        The following symbols are used in this report:

A   longitudinal cross-sectional area of cone, (sq cm)

D_i diffusion coefficient of ith radical at initial temperature

$D_{i,r}$ relative diffusion coefficient of given active radical with
        respect to other radicals

D_m diffusion coefficient of radical at mean combustion-zone
        temperature

E   activation energy, (cal/gram-mole)

h   height of cone, (cm)

k   constant for given fuel

l slant height or length of generating curve, (cm)

n   constant exponent for given fuel

p_i mole fraction or partial pressure of ith radical in burned gas

R   gas constant, $(cal/(gram\text{-}mole)(^\circ K))$

S   lateral surface area, (sq cm)

$T_{av} = (T_0 + T_f)/2$

T_f flame temperature, $(^\circ K)$

T_0 initial mixture temperature, $(^\circ K)$

u   flame speed, (cm/sec)

EXPERIMENTAL PROCEDURE

Apparatus. - The apparatus and the experimental technique used for
the measurement of flame speed were essentially the same as reported in
reference 3. The apparatus is diagrammatically illustrated in figure 1.
In brief, the fuel and the air were metered, mixed, electrically pre-
heated, and burned above a vertical brass tube. For methane, a
120-centimeter length of 15.7-millimeter-inside-diameter tubing was
used; whereas, for ethylene, a 120-centimeter length of 6.3-millimeter-
inside-diameter tubing was used. The smaller tube diameter for
ethylene was necessary because of the higher flashback velocity limit
of ethylene, which results from its higher flame speed. Temperatures
were measured with iron-constantan thermocouples. The gas temperature
at the burner port was periodically checked by locating an aspirating
thermocouple (reference 10) over the center of the port. The gas tem-
peratures at the burner-tube inlet (thermocouple "O") and at the port
(thermocouple "C") were maintained within 10° C of each other. The
parallel-beam shadowgraph system is schematically shown above the burner
port in figure 1.

One modification to the original apparatus consisted in fastening a small resistance heater to the bottom of the burner-lip collar to permit close control of the lip temperature. In the propane-air investigation, the lip temperature was established by the heating due to the flame itself.

Fuels. - The minimum purities claimed by the suppliers of the methane and ethylene were 99.0 and 99.5 percent, respectively. The propane (reference 3) had a minimum purity of 95.0 percent, the major impurities being ethane and isobutane. Laboratory service air containing approximately 0.3-percent water by weight was used.

Computation of flame speed. - Flame speeds were determined from the shadowgraphs by the total-area method, wherein the average normal flame speed is equal to the volume rate of flow of the unburned mixture divided by the surface area of the cone formed by the combustion zone. This surface area S was determined by assuming that the flame surface can be approximated by the relation for conical surfaces of revolution; thus,

$$S = \pi A \, l/h \qquad\qquad (1)$$

A typical shadowgraph is shown in figure 2. The longitudinal cross-sectional cone area A was determined by measuring a magnified image of the shadow cone with a planimeter; the magnified image was obtained by tracing the inner edge of the shadow from the projected image of the shadowgraph. Because of inaccuracies in tracing and using a planimeter, a scatter in the computed points resulted, especially for the tall, slender ethylene flames. The precision at the higher temperatures was 4 percent for ethylene. This scatter was diminished by: (1) determining the average value of A/h for all the computed points at a given temperature, (2) recomputing flame-speed values for one of the points on the basis of the average A/h; and (3) computing the rest of the flame-speed values from the already corrected point by a ratio of cone heights according to the equation $u_2 = u_1 h_1/h_2$. This procedure essentially amounts to the method used in reference 11.

RESULTS AND DISCUSSION

In figure 3, flame speed is plotted against percentage of fuel by volume at each of six initial mixture temperatures ranging from 34° to 344° C. It is assumed that no preflame reaction has occurred during the short preheating period (less than 2 sec) at these temperatures

(reference 7, pp. 406, 411). The stream-flow Reynolds number was approximately 1500 for methane-air mixtures and 2000 for ethylene-air mixtures. Each of the curves shows that the maximum flame speed for a given temperature occurs at a mixture composition richer than stoichiometric. These flame-speed maximums from figure 3 are plotted against temperature in figure 4(a) to show the effect of temperature on the maximum flame speed. The curve from reference 3 for the propane-air mixture is included for comparison. For further comparison, a log-log plot of maximum flame speed against temperature for the three fuels is presented in figure 4(b). None of the curves in figure 4(b) may be exactly represented by a straight line. For an approximate relation, however, an equation of the type

$$u = k \; T_0{}^n$$

may be used. The equations, found by the least-squares method from the points plotted in figure 4(b) (based on the inner edge of the shadow) for the three fuels, are:

For methane,

$$u = 0.000780 \; T_0{}^{1.89}$$

for propane,

$$u = 0.00246 \; T_0{}^{1.72}$$

and for ethylene,

$$u = 0.00971 \; T_0{}^{1.565}$$

These values should not be used for extrapolation to higher or lower temperatures until further experimental data are available.

In figure 5, the percentage increase in maximum flame speed, referred to the flame speed at 34° C, is plotted against temperature. (The value for propane at this temperature was obtained by interpolation from fig. 3 of reference 3.) The flame speeds of these three fuels are again seen to be affected by temperature in the decreasing order, methane, propane, and ethylene.

Flame speeds based on outer edge of shadow. - As indicated in refer-
ences 9 and 12, the maximum density gradient is more nearly represented
by the outer edge of the shadow than by the inner edge, because of the
manner in which the shadow of a flame cone is produced. If the locus
of maximum density gradient is taken to correspond to the flame front,
then absolute values of flame speed should be based on the outer edge
of the shadow. In order to obtain correction factors that could be
used to convert the flame-speed values plotted in the figures of the
present report to values based on the outer edge of the shadow, a group
of points was selected at each temperature for each fuel and was recom-
puted on the new basis. Each group consisted of one point representing
the leanest mixture studied, one point near the composition for maximum
flame speed, and one for the richest mixture studied. Plots of
18 points so selected for each fuel revealed no trends for the cor-
rection factor with respect to either mixture composition or tempera-
ture; the arithmetic mean value of the factors for all 18 points for a
given fuel was therefore considered to be the best value over the ranges
of composition and temperature studied. Inasmuch as all data points for
one fuel would then be corrected by the same constant factor for that
fuel, such correction would not change the relative effects of tempera-
ture on flame speed shown in figures of this report; that is, it would
merely shift the ordinate log scale in figure 4(b) and compress the
ordinate scales in the remaining figures. The empirical equations
obtained from figure 4(b) could therefore be converted to give values
based on the outer edge of the shadow by multiplying by the constants
0.900, 0.885, and 0.849 for methane, propane, and ethylene, respec-
tively. Values based on the inside edge of the shadow are presented
herein because the required measurements were more easily and pre-
cisely made on this basis and because the relative effect of temperature
on flame speed was unaffected.

The arithmetic mean values of the correction factors for the three
fuels are presented in table I. The maximum flame speed at 25° C was
obtained for each fuel by extrapolation from figure 4(a) in order to
compare the value with values obtained by other investigators who used
shadow-cone, visible-cone, and tube measurements (references 3, 8, 9,
and 13 to 16). The agreement among corrected shadow-cone, visible-cone,
and tube measurements for methane and propane is good. The poorer
agreement between various methods and investigators for ethylene is
probably due, in part, to the greater uncertainties in measurements
of the more extreme flame shapes encountered with ethylene in both
Bunsen burner and tube methods.

Comparison of experimental data with relative values predicted by theoretical equations. - It is shown in reference 3 that, for the purpose of predicting the relative effect of temperature on flame speed, the thermal-theory equation of Semenov (reference 4), for a bimolecular reaction controlling, might be reduced to the expression

$$u \propto \sqrt{T_f^{4.9} T_0^2 \; \frac{e^{(-E/RT_f)}}{(T_f - T_0)^3}} \tag{2}$$

The reduction of the Semenov equation to expression (2) involves the assumption that the relations between the physical properties and the temperature for the mixture are reasonably near those for air.

In a similar manner, the thermal-theory equation for unimolecular reaction controlling (reference 4) may be reduced to the following expression:

$$u \propto \sqrt{T_f^{3.83} T_0^2 \; \frac{e^{(-E/RT_f)}}{(T_f - T_0)^2}} \tag{3}$$

The square-root law of Tanford and Pease in the form presented in reference 6 was also considered for the purpose of predicting the relative effect of temperature on flame speed in reference 3. The reduced expression presented in reference 3 is

$$u \propto \sqrt{\left(\sum_i p_i D_{i,r}\right) T_0^{1.67} \; T_{av}^{-1}} \tag{4}$$

where

$$\sum_i p_i D_{i,r} = 6.5 \; p_H + p_{OH} + p_O$$

2144

In arriving at expression (4), it was assumed that the number of molecules per unit volume of gas at some mean temperature L, should be inversely proportional to T_{av}. In reference 5, however, Tanford and Pease apparently intended the mean temperature to be chosen nearer to and perhaps proportional to the flame temperature, for example, 0.7 T_f. The diffusion coefficients were also assumed to be proportional to the square of the absolute temperature, rather than to the 1.67 power used in reference 3. Cancellations of temperature effects involving the two-power relation were made in the process of substituting the diffusion coefficient of radicals at the initial temperature D_i for the diffusion coefficient of radicals at the mean combustion-zone temperature D_m (reference 5); these cancellations resulted in the equation presented in reference 6. If, instead, the temperature dependence $D \propto T^{1.67}$ is applied to the D_m in the derivation (reference 5) rather than to D_i in the final equation as in reference 3, and if $L \propto T_f^{-1}$ is substituted, the revised expression is

$$u \propto \sqrt{\left(\sum_i p_i D_{i,r}\right) \frac{T_0^2}{T_f^{1.33}}} \qquad (5)$$

Comparisons of the relative effects of initial temperature on flame speed as predicted by the reduced equations (2), (3), and (5) for methane, propane, and ethylene are presented in figures 6(a), 6(b), and 6(c), respectively. Each of the curves was plotted by computing flame speeds at various temperatures relative to the experimental value of maximum flame speed at room temperature. The experimental results are represented by the dashed curves.

The activation energies and the flame temperatures used in plotting the theoretical curves in figure 6 are presented in table II. The flame temperatures are based on sodium D-line measurements of flame temperatures of mixtures at room temperature (reference 17). The relations for the change in flame temperature ΔT_f with change in initial temperature ΔT_0 were determined from adiabatic flame-temperature calculations by the method of reference 18. Equilibrium radical concentrations needed for the square-root-law curves were calculated by the graphical method of reference 19 and are presented in table III. For each of the fuel-air mixtures (air containing 0.3-percent water by weight), the radical concentrations were calculated for a series of arbitrary temperatures, which included the range of flame temperatures

considered. Intermediate values of radical concentrations corresponding to specific flame temperatures, which in turn corresponded to specific initial temperatures, were obtained from table III by logarithmic interpolation. Although the radical concentrations for methane-air flames in table III were computed for a fuel concentration of 10.0 percent by volume, whereas the flame-speed maximums in figure 3 occurred at approximately 10.5 percent methane, it can be shown that the curves in figures 6 and 7 would be insensitive to this small change in concentration, because the flame speeds at a concentration of 10.0 percent are very near the maximum values.

The curves in figure 6 show that both the expressions based on the thermal theory and the expression based on a diffusion theory predict the relative effect of initial mixture temperature on maximum flame speed within 20 percent. For methane and propane, the thermal-theory curves are in somewhat better agreement with the experimental results than are the square-root-law curves; whereas for ethylene, the square-root-law curve is in as good, or better, agreement with the experimental results.

It must be emphasized that even qualitative observations regarding the ability of one or the other of the theories to predict the effect of initial temperature on flame speed are subject to the assumptions made in deriving both the original equations and the reduced forms and to the choices of values for E, T_f, and ΔT_f. The effects of using different values of E, T_f, and ΔT_f for propane flames is discussed in reference 3. For example, it could be shown that using $E = 25$ kilocalories per gram-mole, $T_f = 2390^\circ$ K at $T_0 = 305^\circ$ K, and $\Delta T_f = 0.45 \Delta T_0$ for propane would give predicted increases that were approximately 17 percent low by the thermal-theory bimolecular equation and 17 percent low by the square-root law. It is assumed herein that the variation of B_i, a term that appears in the square-root law to allow for radical recombination, with initial temperature is relatively small and would not appreciably affect the curves in figure 6. The temperature dependence of k_i, the rate constant which appears in the square-root law for interaction between the ith radical and the combustible material, has been neglected. Constant values of k_i were used for hydrogen, carbon monoxide, and methane flames in reference 6, where the variations in flame temperature are of the same order of magnitude as those considered herein. If the temperature dependence of k_i is represented by $e^{(-E/RT_f)}$, the temperature effect on flame speed due to k_i will be small, provided that the activation energy for the radical-hydrocarbon reaction is small. For example, using an activation

2144

energy of 7 kilocalories per gram-mole (reference 6), the relative
increases in flame speed predicted by the square-root law for methane,
propane, and ethylene would be raised approximately 8 percent at an
initial temperature of 344° C and less at lower initial temperatures.

The relative merits of the theories could be better assessed if
reliable data for the effect of pressure on flame speed were available.
The thermal-theory equations presented in reference 4 predict that for
a unimolecular reaction, the flame speed should be inversely propor-
tional to the square root of the absolute pressure; whereas, for a
bimolecular reaction, the flame speed should be independent of pres-
sure. The square-root law predicts that flame speed should vary
approximately inversely as the fourth root of the pressure (refer-
ence 6). If one of the theories could be shown to be the more con-
sistent in predicting both pressure and temperature effects, it would
be strengthened considerably. Although some pressure data exist with
which this precept might be tested, conflicting trends for the varia-
tion of flame speed with pressure for a given fuel have been reported
by different investigators, or by the same investigator using different
experimental methods, which indicates that some of these data were
influenced by the experimental apparatus. For example, in reference 20
the flame speed of ethylene measured by a Bunsen burner method was
found to be inversely proportional to the fourth root of pressure;
whereas, according to reference 21 the flame speed of ethylene measured
by a soap-bubble method was found by the same investigator to be inde-
pendent of pressure.

Correlation of flame speeds with active-radical concentrations. -
A correlation between flame speed and $\sum_i p_i D_{i,r}$ for ethylene-air
mixtures of various compositions at room temperature is found in refer-
ence 9. In figure 7(a), the maximum flame speeds from figure 4 are
plotted against $\sum_i p_i D_{i,r}$ computed at temperatures determined from
table II; in figure 7(b), maximum flame speeds are plotted against com-
puted hydrogen-atom concentrations at these same temperatures; and in
figure 7(c) maximum flame speeds are plotted against hydrogen-atom
concentrations at theoretical flame temperatures obtained from refer-
ence 18. In all cases, straight-line correlations are obtained. The
equations of these straight lines are given on the figures. The fact
that the methane and propane points fall on a common line in fig-
ure 7(a) and 7(b) may be a fortuitous result of the choices of measured
flame temperatures, inasmuch as they do not fall on a common line in
figure 7(c), where theoretical flame temperatures were used. The fact

that the ethylene line is different in all cases was not too unexpected
in view of the anomalous behavior of ethylene in a similar correlation
in reference 8, in which flame speed was plotted against $\sum_{i} p_i D_{i,r}$ for
a large number of fuels at room temperature.

The curves of figure 7 indicate that, at least for the three fuels
studied, the maximum flame speed of a gaseous fuel may be accurately
determined over a considerable range of initial mixture tempera-
ture when the experimental values at two temperatures are known and
sufficient data exist to compute the adiabatic flame temperatures, and
hence, the equilibrium hydrogen-atom concentrations. It is recognized
that the slopes of the correlation lines in figure 7 are much steeper
than those shown in the correlations in references 8 and 9. No explana-
tion of the differences in the slopes is offered at the present time.
Further experiments and calculations are indicated, the results of which
may give clews as to the controlling mechanism of flame propagation
under various conditions.

SUMMARY OF RESULTS

An investigation of the effect of initial mixture temperature on
the laminar flame speeds of methane-air and ethylene-air mixtures,
together with earlier work with propane-air mixtures, gave the fol-
lowing results:

1. The flame speeds of methane, propane, and ethylene increased
with initial mixture temperature at an increasing rate. The percentage
change in flame speeds was affected by temperature in the decreasing
order, methane, propane, and ethylene. Although none of these gases
showed maximum flame speed u to be exactly proportional to a power
of temperature T, approximate equations for flame speed in centi-
meters per second (based on the inner edge of the shadow cast by the
cone) for use in the temperature range $34°$ to $344°$ C were:

For methane,

$$u = 0.000780 \ T_0^{1.89}$$

for propane,

$$u = 0.00246 \ T_0^{1.72}$$

and for ethylene,

$$u = 0.00971 \ T_0^{1.565}$$

2144

2. Flame-speed values based on the outer edge of the shadow cast by the Bunsen cone (total-area method) were close to those based on both visible Bunsen cone measurements and tube measurements for methane and propane, but the variation in values obtained by the three methods was greater for ethylene. For each fuel, a factor was determined to allow conversion of values based on the inner edge of the shadow to values based on the outer edge of the shadow; the conversion factors were constant with respect to both temperature and composition, within the accuracy of the measurements based on the outer edge of the shadow. The empirical equations presented in result (1) could therefore be converted to give values based on the outer edge of the shadow by multiplying by the constants 0.900, 0.885, and 0.849 for methane, propane, and ethylene, respectively.

3. Both the thermal-theory equations presented by Semenov and the square-root law of Tanford and Pease (diffusion theory) may be used to predict within 20 percent or better the relative effect of initial temperature on flame speed for the gases studied. Of the two theories, the thermal theory gave somewhat better predictions for methane and propane, whereas the square-root law was as good, or better, for ethylene; this qualitative observation was subject, of course, to the assumptions made in applying the equations.

4. Very good straight-line correlations between maximum flame speed and either the hydrogen-atom concentration alone or the summation of the effective relative concentrations of hydrogen atoms, hydroxyl radicals, and oxygen atoms were found for the three fuels. Equally good correlations were obtained using either flame temperatures based on sodium D-line measurements or adiabatic flame temperatures. The slopes of the correlation lines were steeper than those reported elsewhere in investigations of the effects of mixture composition and fuel type on flame speed. Further experimental and theoretical investigation may show why the slopes were different and give a better insight into the mechanisms involved in flame propagation.

Lewis Flight Propulsion Laboratory,
    National Advisory Committee for Aeronautics,
        Cleveland, Ohio, February 20, 1951.

REFERENCES

1. Childs, J. Howard, McCafferty, Richard J., and Surine, Oakley W.: Effect of Combustor-Inlet Conditions on Performance of an Annular Turbojet Combustor. NACA Rep. 881, 1947. (Formerly NACA TN 1357.)

2. Mullen, James W., II, Fenn, John B., and Garmon, Roland C.: Burners for Supersonic Ram-Jets. Ind. and Eng. Chem., vol. 43, no. 1, Jan. 1951, pp. 195-211.

3. Dugger, Gordon L.: Effect of Initial Mixture Temperature on Flame Speeds and Blow-Off Limits of Propane - Air Flames. NACA TN 2170, 1950.

4. Semenov, N. N.: Thermal Theory of Combustion and Explosion. III - Theory of Normal Flame Propagation. NACA TM 1026, 1942.

5. Tanford, Charles, and Pease, Robert N.: Theory of Burning Velocity. II. The Square Root Law for Burning Velocity. Jour. Chem. Phys., vol. 15, no. 12, Dec. 1947, pp. 861-865.

6. Tanford, Charles: The Role of Free Atoms and Radicals in Burner Flames. Third Symposium on Combustion and Flame and Explosion Phenomena, The Williams & Wilkins Co. (Baltimore), 1949, pp. 140-146.

7. Jost, Wilhelm: Explosion and Combustion Processes in Gases. McGraw-Hill Book Co., Inc., 1946.

8. Simon, Dorothy Martin: Flame Propagation. III. Theoretical Consideration of the Burning Velocities of Hydrocarbons. Jour. Am. Chem. Soc., vol. 73, no. 1, Jan. 1951, pp. 422-425.

9. Linnett, J. W., and Hoare, M. F.: Burning Velocities of Ethylene-Air-Nitrogen Mixtures. Third Symposium on Combustion and Flame and Explosion Phenomena, The Williams & Wilkins Co. (Baltimore), 1949, pp. 195-203; discussion by Kurt Wohl, pp. 203-204.

10. Anon.: Temperature. Its Measurement and Control in Science and Industry. Reinhold Pub. Corp., 1941, pp. 847-854.

11. Bollinger, Lowell M., and Williams, David T.: Effect of Reynolds Number in Turbulent-Flow Range on Flame Speeds of Bunsen Burner Flames. NACA Rep. 932, 1949. (Formerly NACA TN 1707.)

2144

12. Grove, J. R., Hoare, M. F., and Linnett, J. W.: The Shadow Cast
    by a Bunsen Flame, Its Production and Usefulness. Trans.
    Faraday Soc., vol. 46, pt. 9, Sept. 1950, pp. 745-755.

13. Andersen, J. W., and Fein, R. S.: Measurement and Correlation of
    Burning Velocities of Propane-Air Flames. CM-552, Dept. Chem.,
    Naval Res. Lab., Univ. Wisconsin, July 20, 1949. (BuOrd
    Contract Nord 9938, Task WIS-1-G.)

14. Calcote, Hartwell F., Barnett, Charles M., and Irby, Moreland R.:
    The Burning Velocity of Various Compounds by the Bunsen Burner
    Method. Paper presented at 116th Meeting Am. Chem. Soc.
    (Atlantic City, N.J.), Sept. 18-23, 1949. (See Abstracts of
    Papers 116th Meeting of Am. Chem Soc., p. 38P.)

15. Harris, Margaret E., Grumer, Joseph, von Elbe, Guenther, and
    Lewis, Bernard: Burning Velocities, Quenching, and Stability
    Data on Nonturbulent Flames of Methane and Propane with Oxygen
    and Nitrogen. Third Symposium on Combustion and Flame and
    Explosion Phenomena, The Williams and Wilkins Co. (Baltimore),
    1949, pp. 80-89.

16. Culshaw, G. W., and Garside, J. E.: A Study of Burning Velocity.
    Third Symposium on Combustion and Flame and Explosion Phenomena,
    The Williams and Wilkins Co., (Baltimore), 1949, pp. 204-209.

17. Perry, John H.: Chemical Engineers' Handbook. McGraw-Hill Book
    Co., Inc., 2d. ed., 1941, p. 2410.

18. Hottel, H. C., Williams, G. C., and Satterfield, C. N.: Thermo-
    dynamic Charts for Combustion Processes, Pt. I. John Wiley and
    Sons, Inc., 1949.

19. Huff, Vearl N., and Calvert, Clyde S.: Charts for the Computa-
    tion of Equilibrium Composition of Chemical Reactions in the
    Carbon-Hydrogen-Oxygen-Nitrogen System at Temperatures from
    2000° to 5000° K. NACA TN 1653, 1948.

20. Linnett, J. W., and Wheatley, P. T.: Effect of Pressure on Velo-
    city of Burning. Nature, vol. 164, no. 4166, Sept. 3, 1949,
    pp. 403-404.

21. Gaydon, A. G., and Wolfhard, H. G.: Low-Pressure Flames and
    Flame Propagation. Fuel, vol. XXIX, no. 1, Jan. 1950,
    pp. 15-19.

2144

TABLE I - CORRECTION FACTORS FOR COMPUTING FLAME SPEEDS BASED ON

OUTER EDGE OF SHADOW AND COMPARISON OF 25° C VALUES WITH

VISIBLE BUNSEN-CONE AND TUBE MEASUREMENTS

Fuel	Correction factor		Flame speed at 25° C (cm/sec)				Flame speed at 340° C (cm/sec)	
	Mean value	Mean deviation	Inner edge	Corrected to outer edge	Visible cone	Tube method (a)	Inner edge (b)	Corrected to outer edge
Methane	0.900	0.017	[b]37.2	33.5	33.3	33.8	147	132
Propane	0.885	0.017	[b]44.9 [d]45.5 [f]46.6	40.8	[c]38.5 [e]41.5	39.0	158	140
Ethylene	0.849	0.027	[b]73.7 [f]74.6 [h]72.0	62.5	[g]60.0	68.3	229	195

[a]Based on total area of flame traveling at uniform velocity inside pyrex tube (reference 8).

[b]Obtained from figure 4(a) by extrapolation or interpolation.

[c]Based on total-area method, center of luminous zone (reference 3).

[d]Total-area value extrapolated to diametral axis of flame; value of 45.0 cm/sec obtained by stroboscopic method (reference 13).

[e]Based on area of cone frustrum (reference 15).

[f]Based on area of upper part of shadow cone only (reference 14).

[g]Based on total-area method (reference 16).

[h]Mean value of number of measurements by angle method at different cone positions (reference 9).

TABLE II – ACTIVATION ENERGIES AND FLAME TEMPERATURES

USED FOR THEORETICAL CURVES

Fuel	E $\left(\dfrac{cal}{gram\text{-}mole}\right)$	T_f (°K) (a)	ΔT_f (b)
Methane	[c]52,000	2150	$0.54\ \Delta T_0$
Propane	[d]38,000	2200	$0.50\ \Delta T_0$
Ethylene	[e]40,000	2250	$0.475\ \Delta T_0$

[a]For $T_0 = 307°$ K, based on sodium D-line measurement (reference 17).
[b]From adiabatic flame-temperature calculations (reference 18).
[c]Unpublished data obtained by A. D. Walsh.
[d]Reference 7, p. 437.
[e]Reference 9.

TABLE III – EQUILIBRIUM RADICAL CONCENTRATIONS BY

GRAPHICAL METHOD[a]

Fuel	Fuel (percent by volume)	T (°K)	Partial pressure, atm$\times 10^3$			$\sum_i p_i D_{i,r} \times 10^3$
			p_H	p_{OH}	p_O	
Methane	10.0	2100	0.274	0.811	0.0221	2.61
		2200	.494	1.76	.0836	5.05
		2300	.862	3.34	.262	9.20
		2400	1.47	5.98	.728	16.26
Propane	4.2	2200	0.430	1.65	0.088	4.53
		2300	.775	2.90	.250	8.18
		2400	1.35	5.20	.720	14.68
Ethylene	7.5	2200	0.665	0.913	0.0321	5.26
		2300	1.12	1.86	.113	9.25
		2400	1.83	3.39	.331	15.52
		2500	2.96	5.78	.857	25.88

[a]Computed for air containing 0.3 percent water by weight (reference 19).

Figure 1. – Diagrammatic sketch of experimental apparatus.
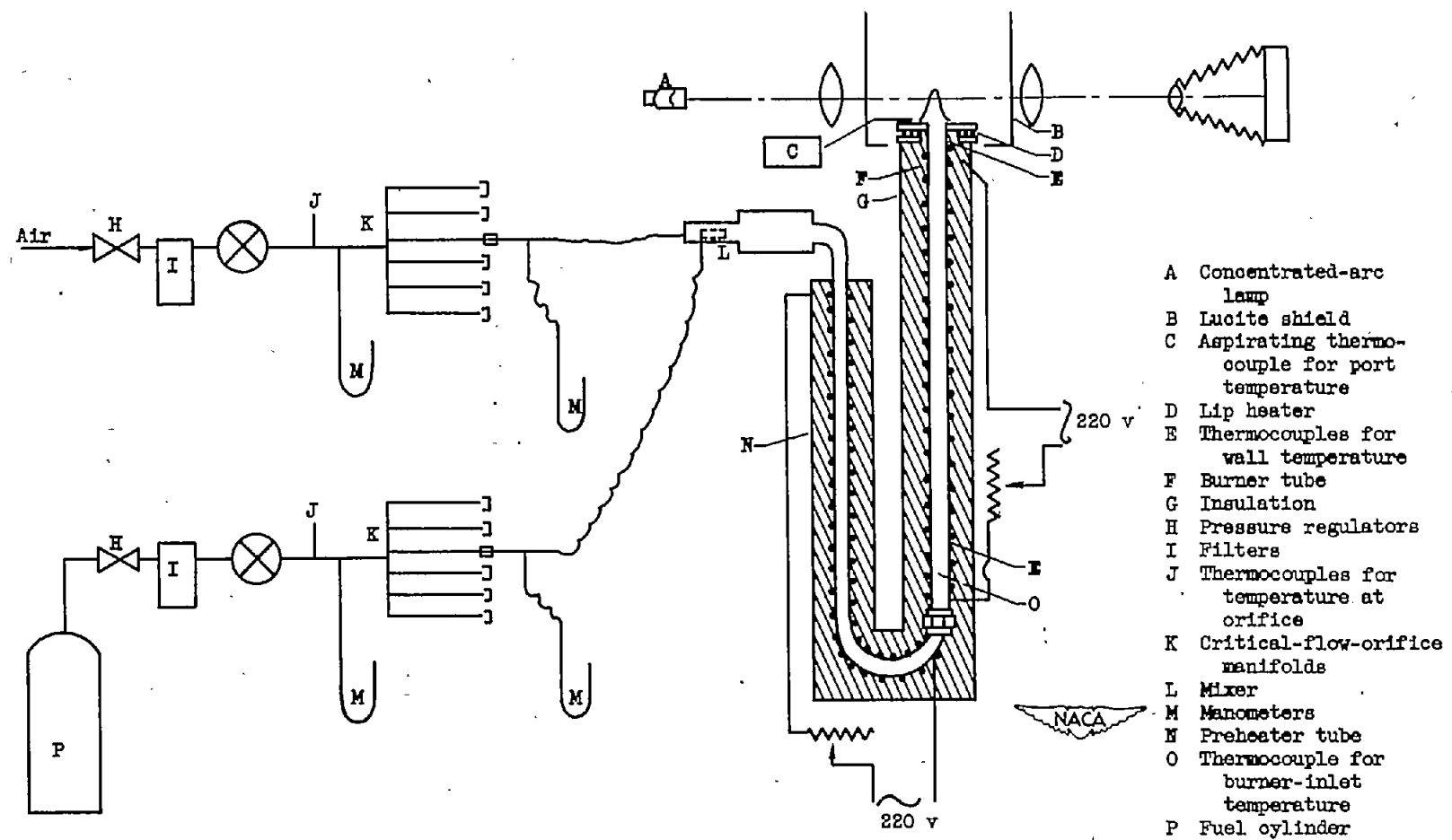
A Concentrated-arc
   lamp
B Lucite shield
C Aspirating thermo-
   couple for port
   temperature
D Lip heater
E Thermocouples for
   wall temperature
F Burner tube
G Insulation
H Pressure regulators
I Filters
J Thermocouples for
   temperature at
   orifice
K Critical-flow-orifice
   manifolds
L Mixer
M Manometers
N Preheater tube
O Thermocouple for
   burner-inlet
   temperature
P Fuel cylinder

Figure 2. - Typical shadowgraph, showing inner and outer edges of shadow cast by Bunsen cone.
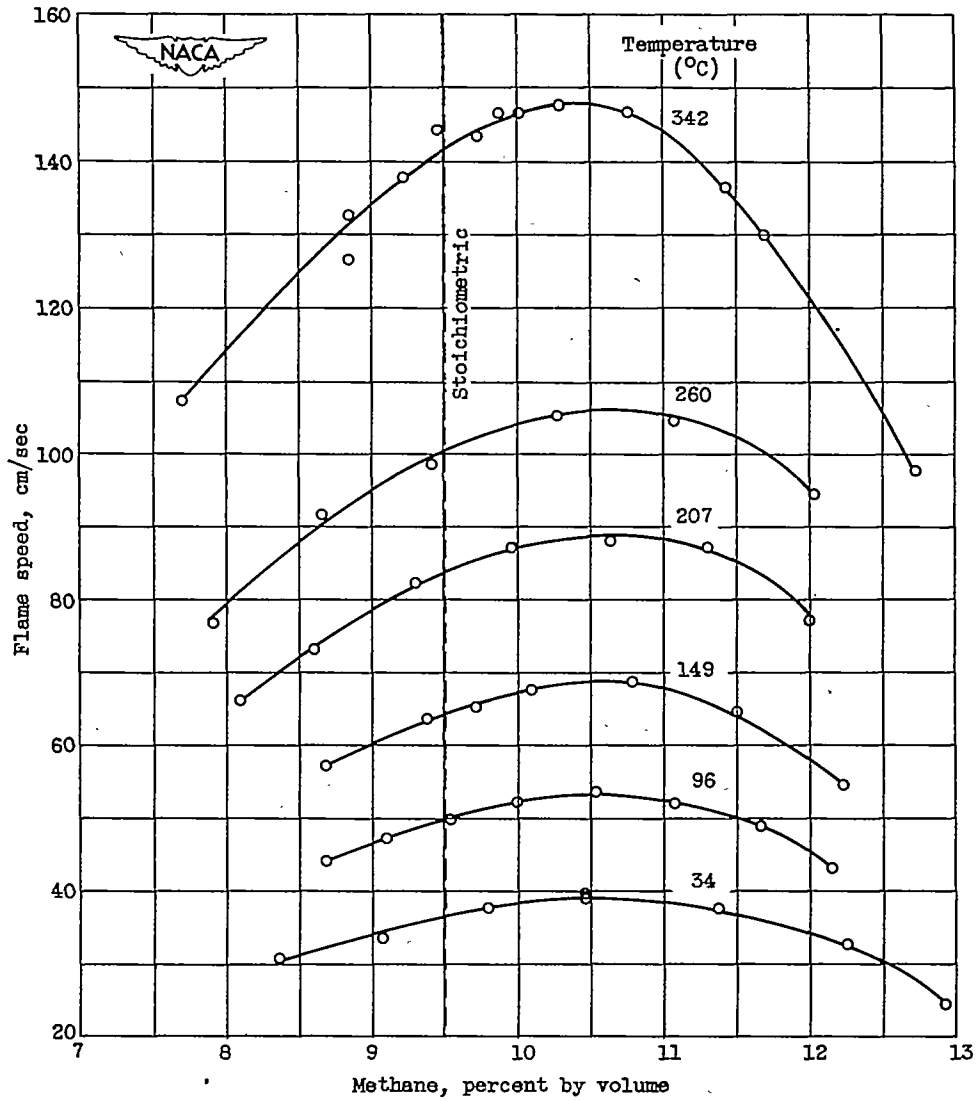
(a)　Methane-air flames.　Tube diameter, 1.57 centimeters; stream-flow
Reynolds number, approximately 1500.

Figure 3. - Flame speed as a function of percentage fuel by volume at
various temperatures.
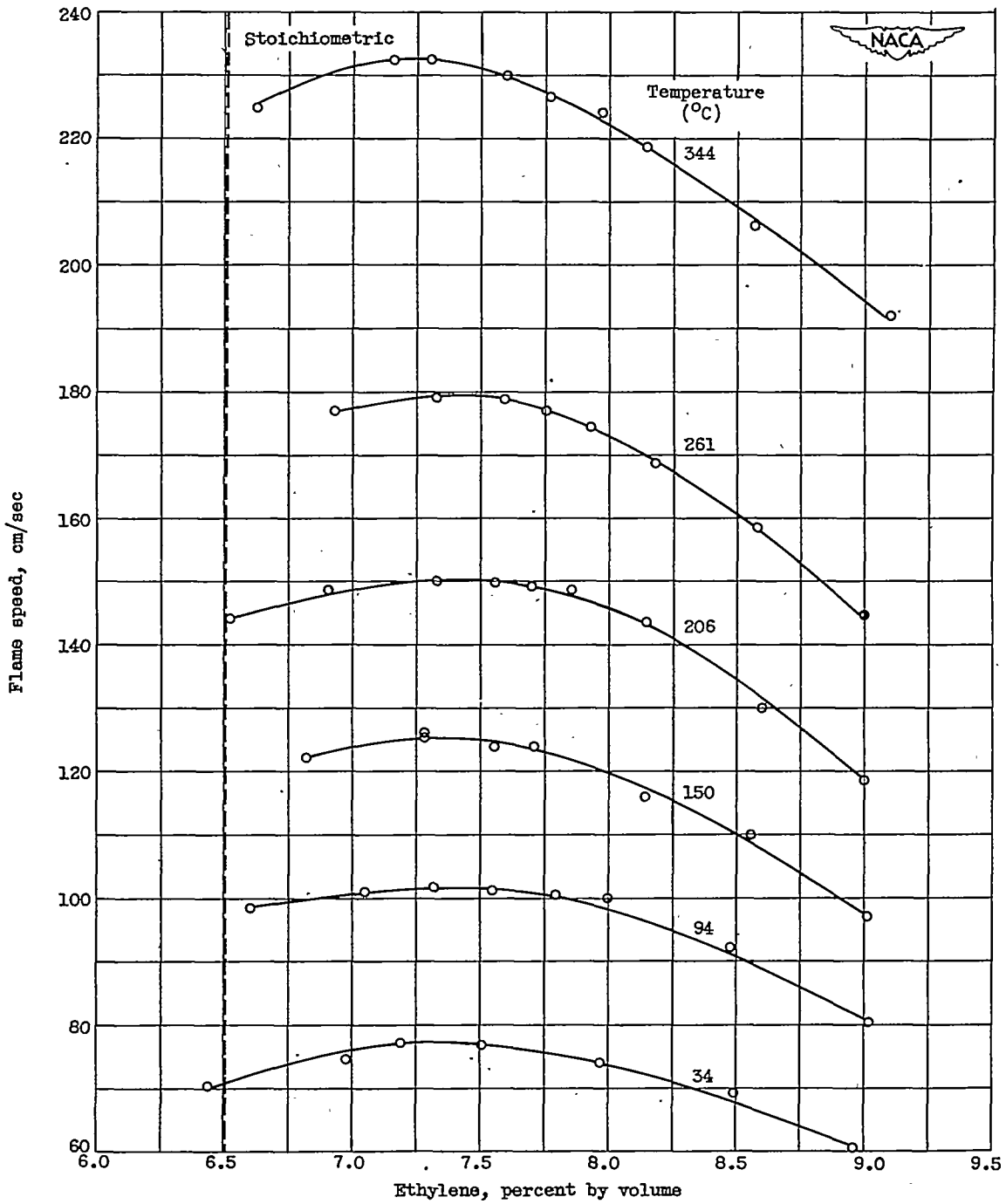
(b) Ethylene-air flames. Tube diameter, 0.631 centimeter; stream-flow Reynolds number, approximately 2000.

Figure 3. - Concluded. Flame speed as a function of percentage fuel by volume at various temperatures.
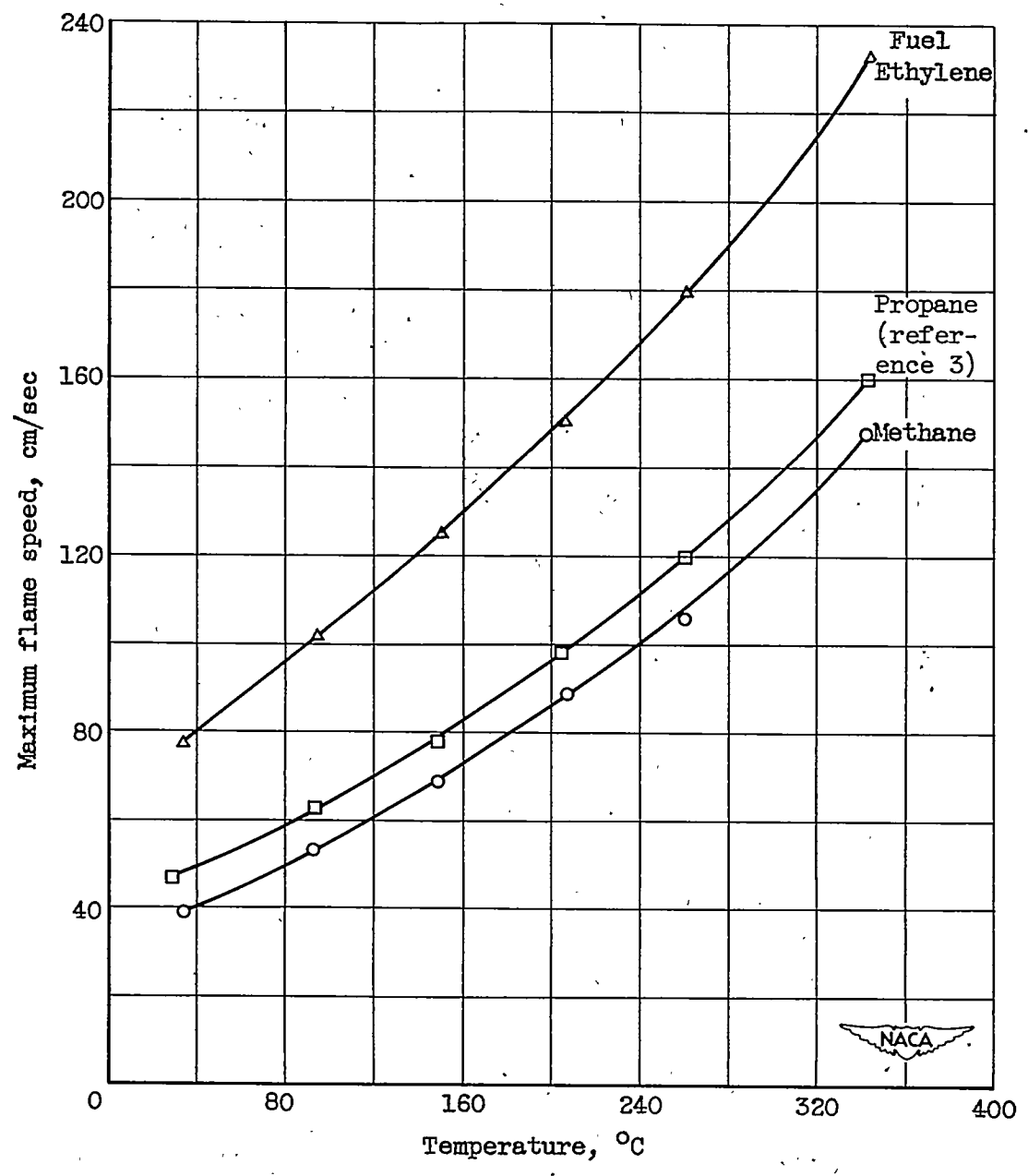
(a) Rectangular coordinates.

Figure 4. - Effect of temperature on maximum flame speed for
methane, propane, and ethylene.
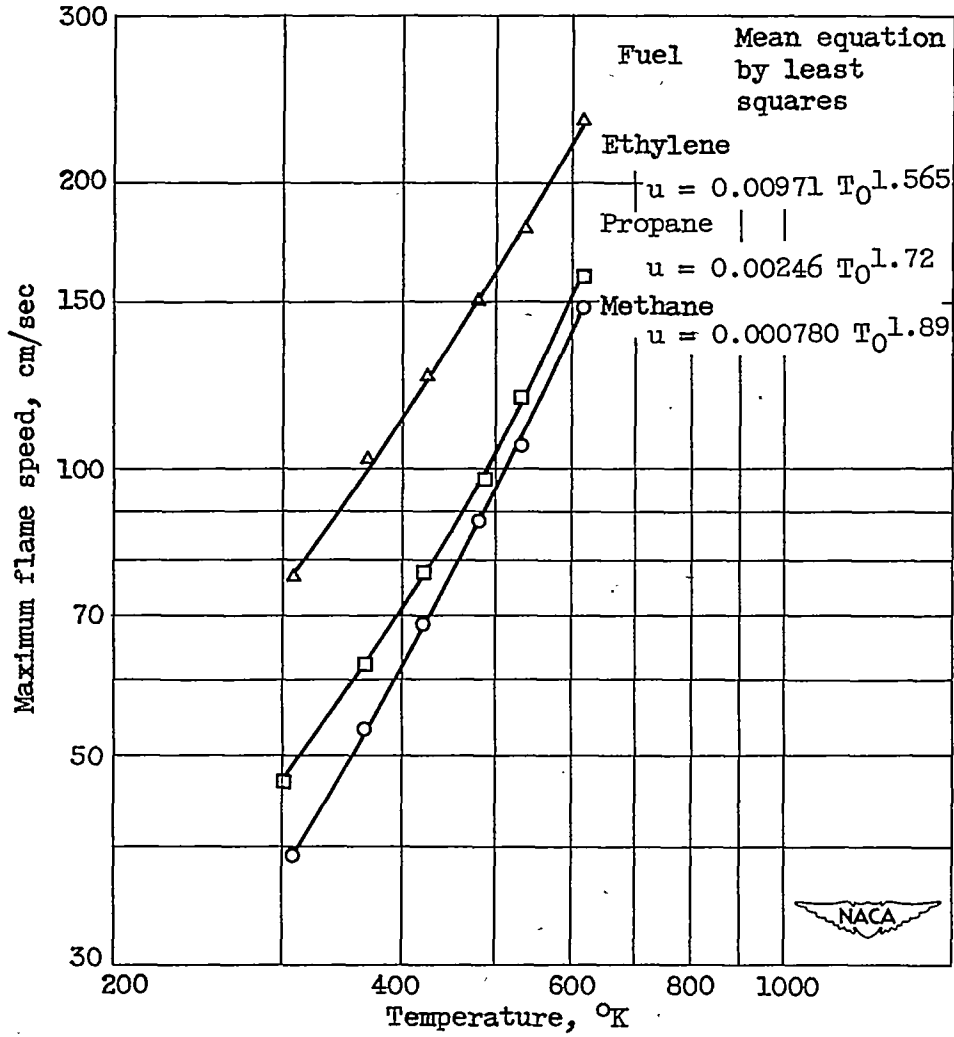
(b) Logarithmic coordinates.

Figure 4. - Concluded. Effect of temperature on maximum flame speed for methane, propane, and ethylene.
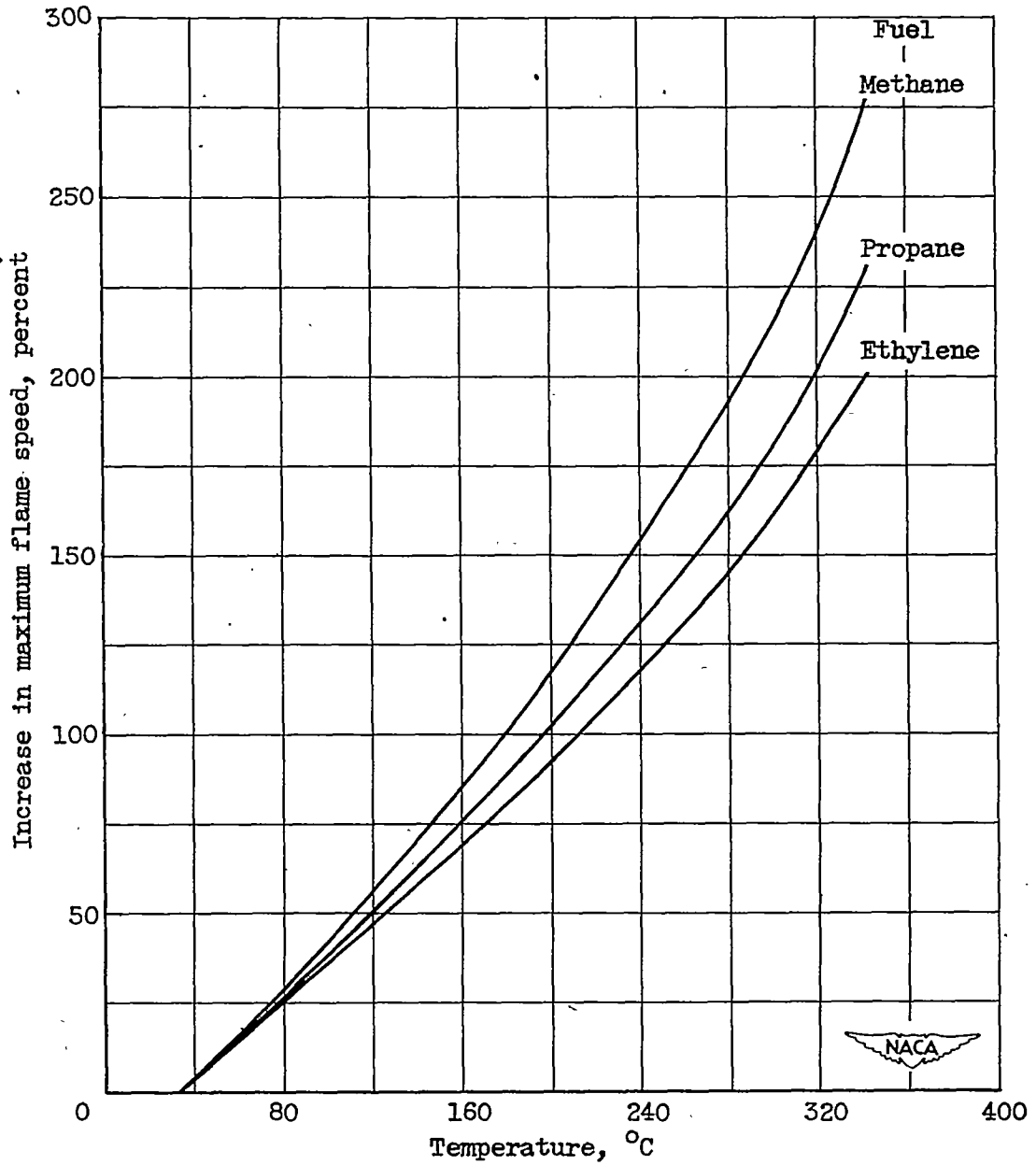
Figure 5. - Percentage increase of maximum flame speed,
referred to flame speed at 34° C, with temperature for
methane, propane, and ethylene.
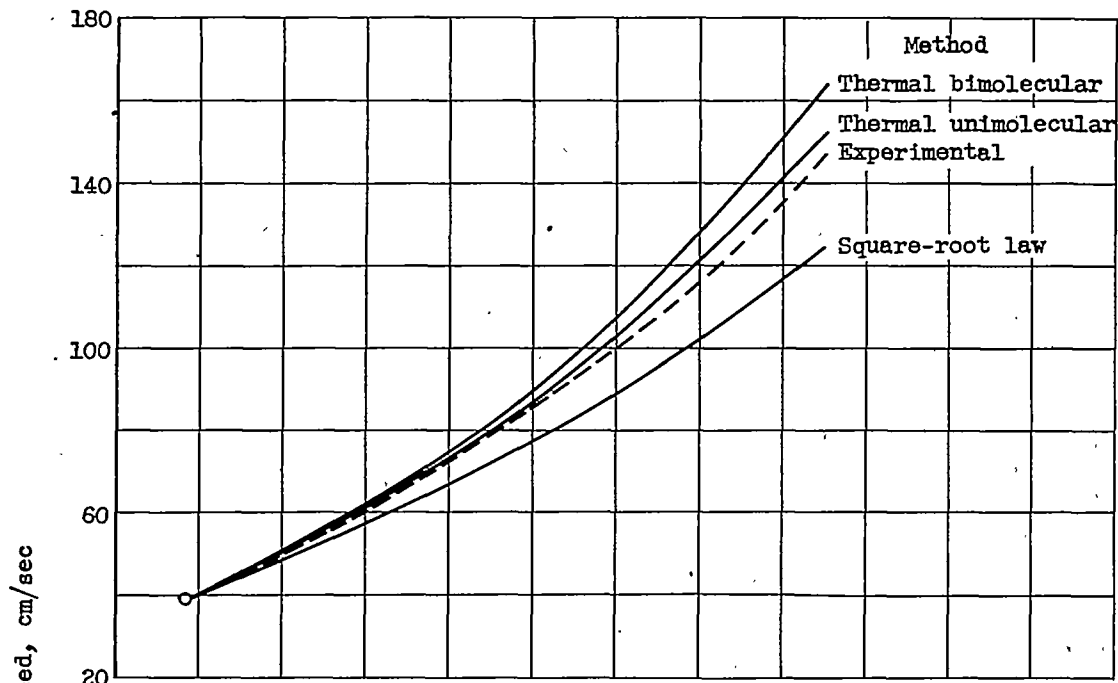
(a) Methane-air flames.
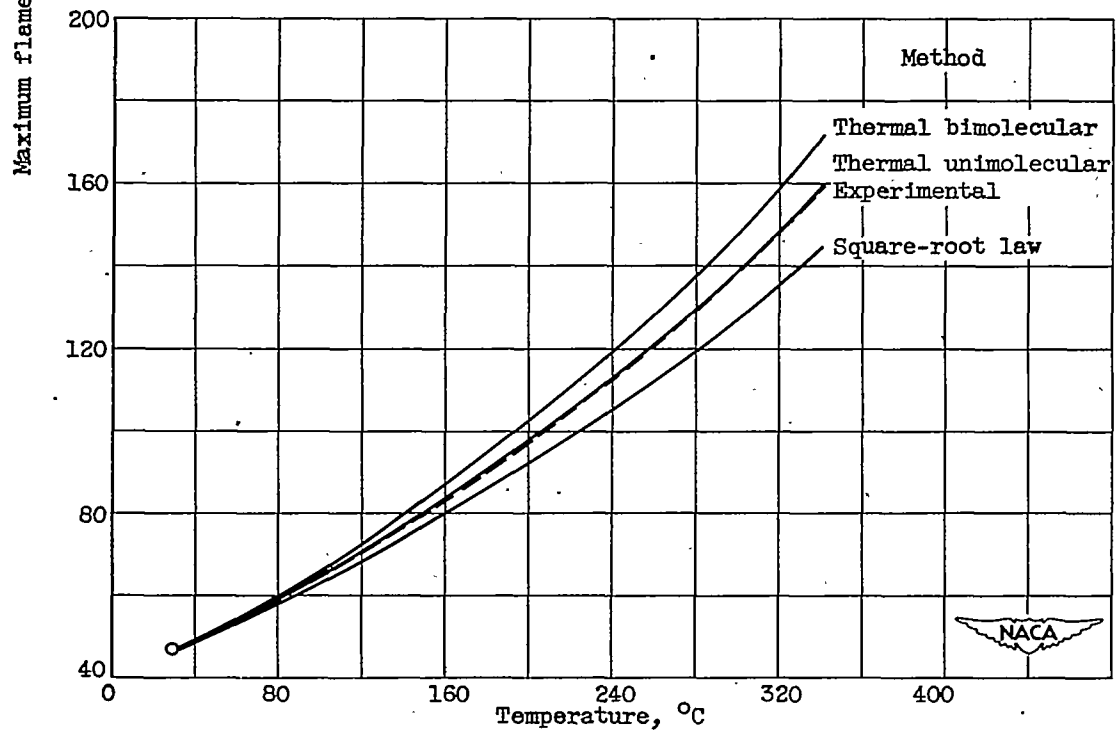
(b) Propane-air flames.

Figure 6. - Effect of temperature on maximum flame speed. Comparison of experimental results with theoretically predicted curves.
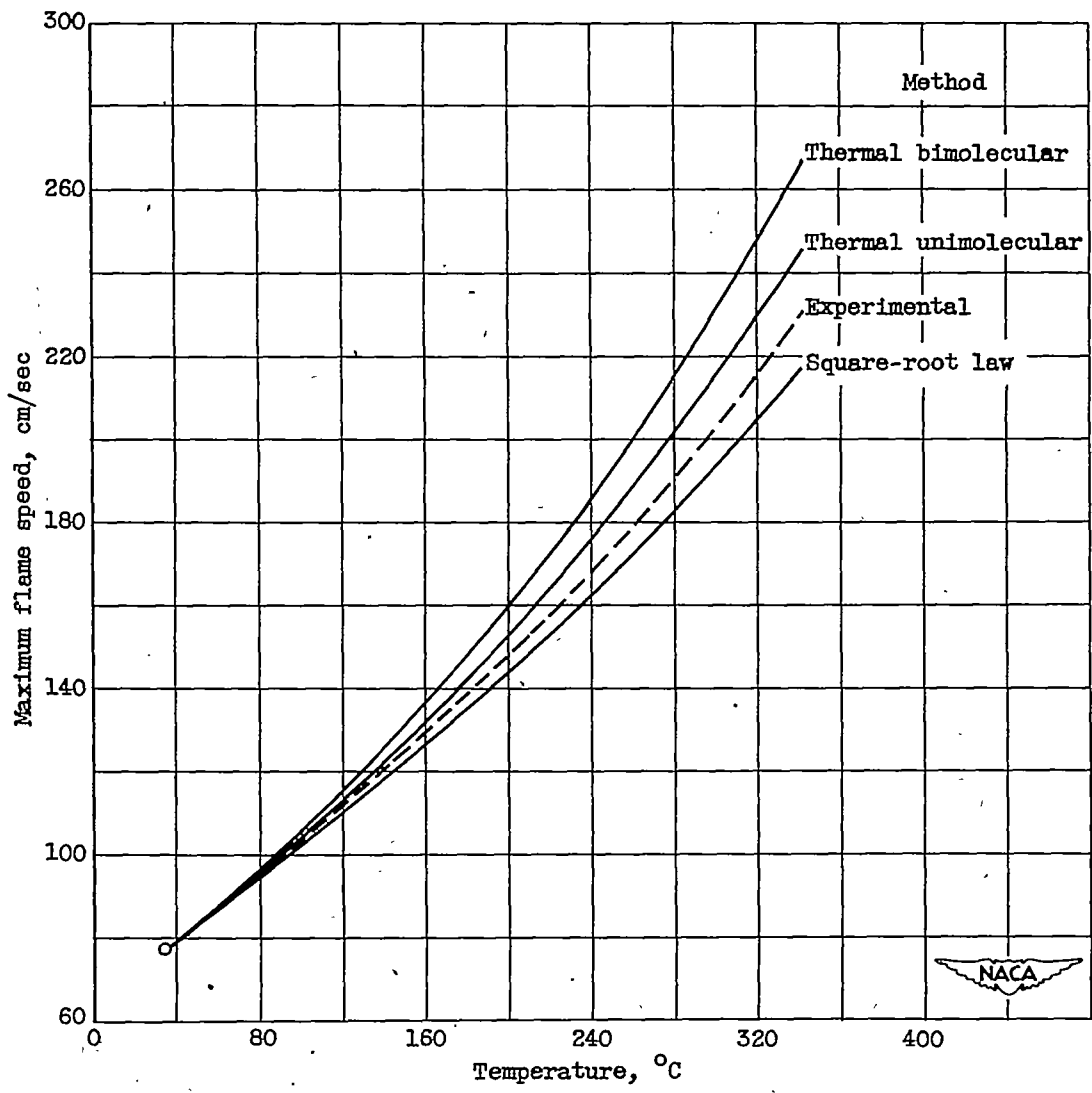
(c) Ethylene-air flames.

Figure 6. - Concluded. Effect of temperature on maximum flame speed.
Comparison of experimental results with theoretically predicted curves.
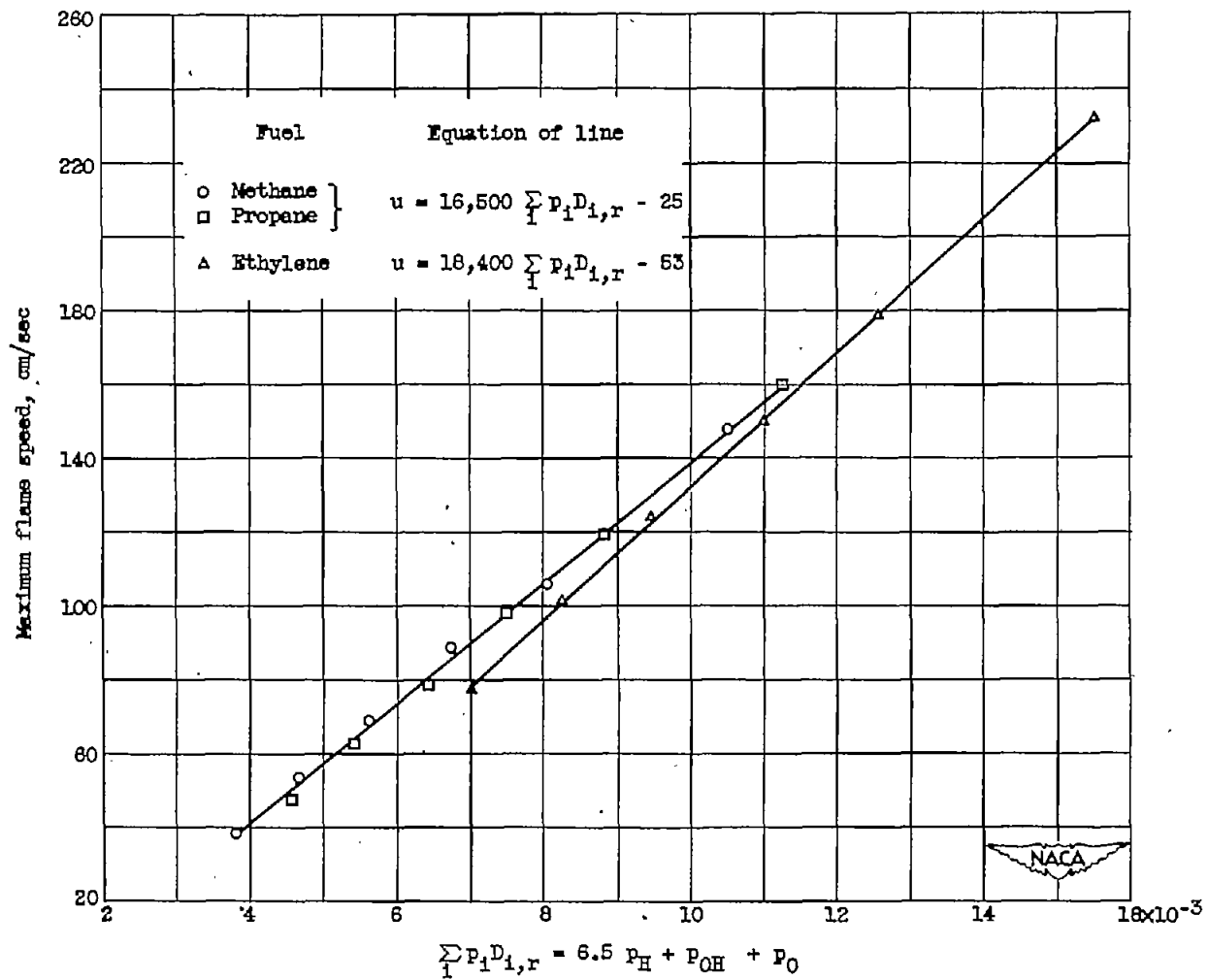
(a) Summation of effective relative radical concentrations, $6.5\ p_H + p_{OH} + p_O$, at flame temperatures based on sodium D-line measurements.

Figure 7. - Correlations between maximum flame speeds and active-radical concentrations.
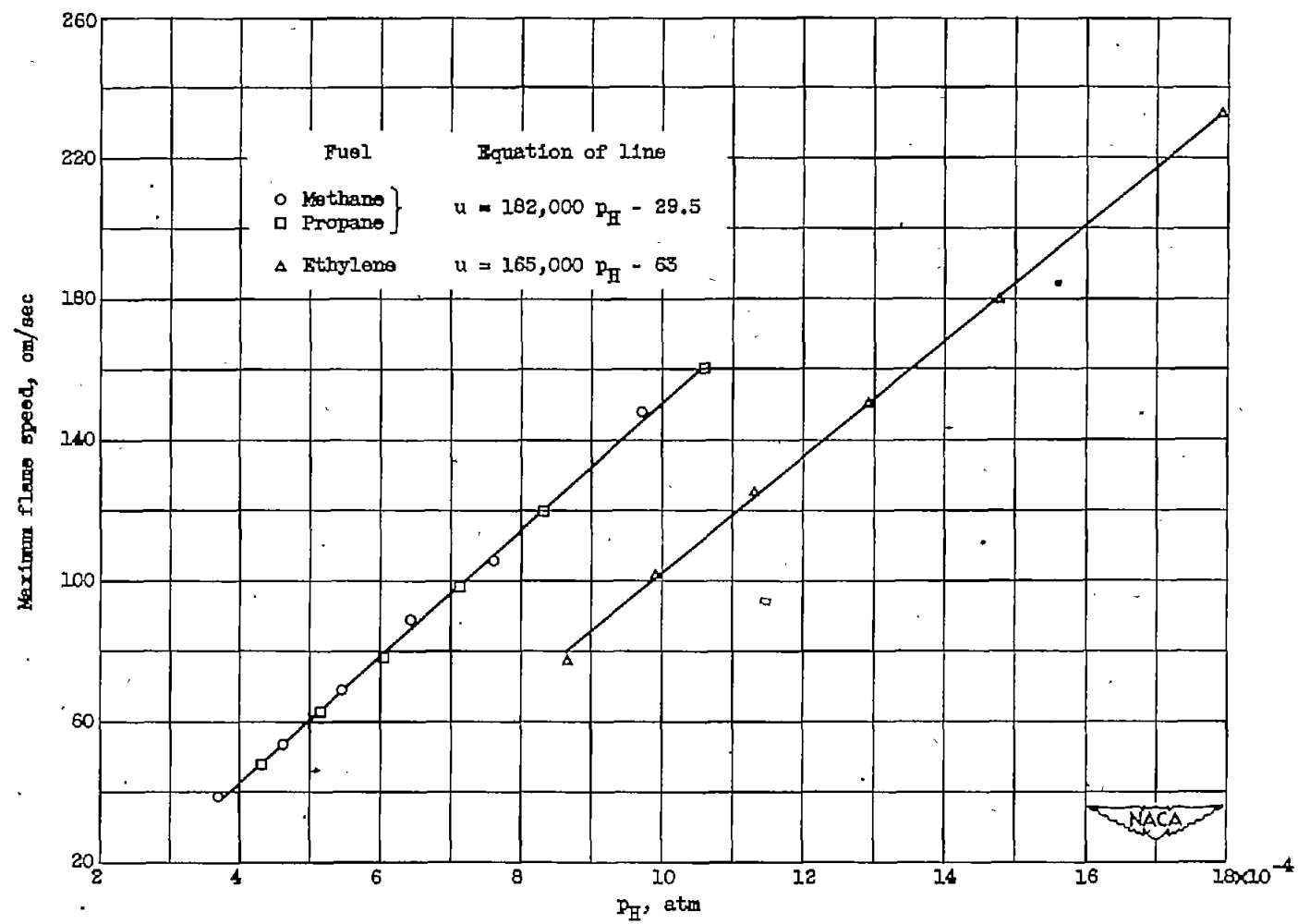
(b) Hydrogen-atom concentration at flame temperatures based on sodium D-line measurements.

Figure 7. - Continued. Correlations between maximum flame speeds and active-radical concentrations.
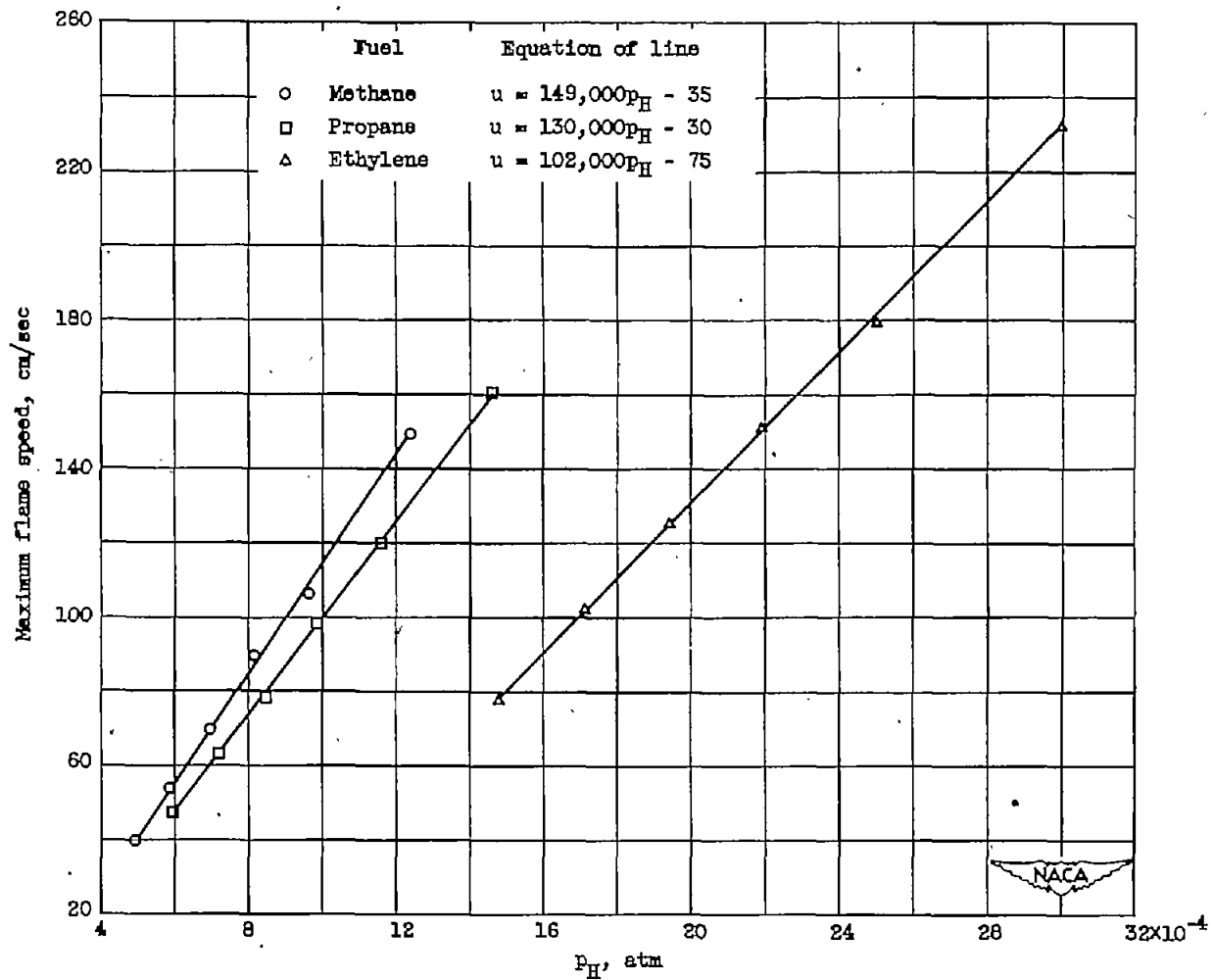
(c) Hydrogen-atom concentration at adiabatic flame temperatures.

Figure 7. - Concluded. Correlations between maximum flame speeds and active-radical concentrations.